ANTENNA PATTERN ANALYSIS -A COMPUTER METHOD

F. M. WOLFF
Engineering Department
Atlantic Research Corporation
The Susquehanna Corporation

Summary This paper describes a digital computer program which is used to calculate certain performance parameters for a telemetry antenna on a flight vehicle. Ground tests of the antenna, or its mockup, are performed and readings taken of the observed gains. This gain pattern is in the form of paper tape which is converted to a computer, acceptable punched are format. The program was written for the IBM 360/65 computer operating under multiprogramming with a variable number of tasks. A visual representation of the pattern is presented and radar tracking site information is displayed in tabular form. Examples of predicted data and flight data are shown.

Introduction Antennae are physical structures which act as an intermediary between guided waves and free-space waves or vice versa[1]. The method by which an antenna performs this intermediary task can be described by certain characteristics; among these are efficiency, radiation pattern, and polarization. Specific interest was focused on polarization and its effect on the antenna radiation pattern, especially insofar as it effected the pattern structure. If antenna patterns were visible, the effect of the perturbation of certain parameters could be more easily studied.

The Scientific Atlanta Corporation developed a method[2] by which data is acquired and the radiation pattern is presented in terms of power per unit solid angle, for a predetermined input power to the antennas. This method and equipment are utilized by a local firm which performs the ground tests under contractual agreements, and prepares the initial data representation namely the paper tapes and array maps. (Figure 1) Each data point in the array represents the magnitude of a vector whose sense was determined from a suitable coordinate system. Thus, the basis was formed for a visual presentation of the radiation pattern.

---

[1] J. S. Korsus, “Antennas, “ McGraw Hill Book Company, Inc. New York, New York, pp 1: 1950

[2] J. S. Hollis, “Antenna Measurements, “ Microwave Journal; Vol 3, No. 2, February 1960.

The data is quite voluminous and an extensive period of time would be required if manual methods of reduction were employed. This, then, formed the incentive and basis for the development of a computerized method of processing the information.

This paper presents the results of that development effort.

The Antenna Gain Factor program was developed at the Missile Systems Division of Atlantic Research Corporation. Development took place under the auspices of the Athena Vehicle program under contract to the U. S. A. F. Advanced Ballistic Reentry Systems Program. In August 1968, effort was initiated on a method of adequately examining the S-Band telemetry antennas used in the Athena research vehicle as well as at the tracking sites along the inland test range between Green River, Utah and White Sands, New Mexico.

The data were obtained from testing methods and procedures developed by the Scientific Atlanta Corporation. The data consisted of punched paper tapes and a representation of the information in array form.

The array containing the test data consists of 16,200 numbers in 90 rows and 180 columns (Figure 1). Each row and column represents a strip, two degrees wide, on the surface of a sphere. Each row represents an aspect angle (θ) of two degrees, where the aspect angle is defined as shown in Figure 2. Similary, the columns or roll angles (ϕ) are defined as shown in Figure 2.

Each element in the array is a number which represents the power ratio in decibels (db) below the isotropic level for that antenna.

If these are considered as vector lengths whose sense is θ degrees from the roll axis and ϕ degrees from the pitch axis, then these vectors will describe a spheroid shape which can be considered to have a volume and a surface area.

Let $G_{\theta\phi}$ represent the vectors in the array, then the average vector magnitude would be:

$$\frac{\sum_{\theta_i=0}^{180^\circ} \sum_{\phi_i=0}^{360^\circ} G'_{\theta\phi}}{90 \times 180} \text{ ; where } G' \text{ is antilog } G \qquad (1)$$

The projection of the sphere onto an X-Y plot tends to foreshorten the polar region and compensations must be made for this. Equation (1) becomes:

$$G_{avg} = 10 \, Log_{10} \left[\frac{\sum_{\theta_i=0}^{180°} \sum_{\phi_i=0}^{360°} G'_{\theta\phi} \, Sin \, \theta_{avg}}{16,200 \times \sum_{\theta_i=0}^{180°} \left[Sin \, (\theta_{avg}) \right]} \right] \tag{2}$$

Similarly, the average gain over the forward, mid, and after thirds of the spherelike antenna pattern are calculated.

The antenna efficiency is defined as the ratio of gain to directivity. However, this program was designed for a particular application where directivity was not required, hence the classical efficiency is not calculated. There exists a further hinderance to calculating efficiency, the patterns most frequencly analyzed were tested under polarized, reception. The total gain for such instances is the vector sum of the two polarizations (i.e., left and right). For the instance where E_θ or E_ϕ polarization is used, the phase angle must be considered unless perpendicular antennae were used and each polarization accomplished by maximizing gain at each θ and ϕ grouping.

The numeric value shown as antenna efficiency is a relative index of the ratio of propagated power to applied power. Test data was taken for mockups of flight equipment, where the antenna was viewed through various materials, of different dielectric constants, which were to be used as heat shields.

$$\eta = \left[(G'_{avg} + G'_{iso}) / G'_{iso} \right] \times 100 \tag{3}$$

One of the requirements was to calculate the percentage of area, of the irregular spheroid, which was above or below a given reference. The . reference was specified as a sphere whose radius was equivalent to a given db level.

$$A_{\ell gr} = \sum_{\theta_i=0}^{180°} \sum_{\phi_i=0}^{360°} R_i \, \Delta\theta_i \, \Delta\phi_i \, Sin \, (\theta i_{avg}) \tag{4}$$

where R_i = unit radius

The sum is computed for all points where

$$G_{\theta\phi} \geq G_{iso} - DB_{ref} \qquad -16 \leq DB_{ref} \leq -1 \tag{5}$$

The information discussed above is displayed in printed form as shown in Figure 3.

Radar Subroutine This routine provides information for tracking stations along the flightpath of a ballistic vehicle. The routine depends, for its input information, on the output of a six-degree-of-freedom (SDF) trajectory program. The SDF program produces a magnetic tape with a time history of aspect angle, roll angle, and slant range[3] for a given vehicle and a given radar site. The routine calculates average gain, received intensity and signal-to-noise ratio for this time history.

Two vehicle conditions are considered. First, in the event that the vehicle is rotating about the roll axis, evaluation of the exact pointing angle is difficult , to obtain due to the spin rates involved. The trajectory program in its simulation will always be in the same attitude, whereas the vehicle operating in a changing environment does not always present the same view. It was, therefore, assumed that examining the entire "roll strip" at the particular aspect angle present a fair approximation. The minimum, maximum, and average gain are determined for this "strip" and the average gain is used to calculate received intensity and signal-to-noise ratio. Second, in the event the vehicle is not spinning, the roll angle and aspect angle are used to determine the average gain from the data array. Interpolation is used where applicable and the gains are assumed to be linear over a 2-degree increment. A sample printout is shown in Figure 4.

A typical formulation is shown:

The magnitude of the power received by an antenna from an incident wave whose intensity is given in watts per square meter, is equal to the product of the wave intensity and the effective area of the receiving antenna.

$$P_R = \frac{W}{M^2} \times A \qquad (6)$$

The effective area of an isotropic receiving antenna is equal to

$$A = \frac{\lambda^2}{4\pi} \qquad (7)$$

where $\lambda = c/f$

$c = 300 \times 10^6$ meters/sec

f = frequency in cps

The power received by an isotropic receiving antenna is

$$P_R = \frac{W}{M^2} \times \frac{\lambda^2}{4\pi} \text{ watts} \qquad (8)$$

---

[3] Slant Range. Line of sight distance between the receiver antenna and the vehicle.

or, in dbm

$$P_{Rdbm} = 10 \, Log_{10} \left[\frac{W}{M^2} \times \frac{\lambda^2}{4\pi} \times 10^3 \right] \quad (9)$$

The received signal strength in dbm by an antenna having a gain (G) in decibels relative to an isotropic antenna is

$$P_{RDBM} = G + 10 \, Log_{10} \left[\frac{W}{M^2} \times \frac{\lambda^2}{4\pi} \times 10^3 \right] \quad (10)$$

Receiving gains at a particular radar site have been reported as 39 db at a frequency of 2250 MHz

$$\frac{\lambda^2}{4} = \left[\frac{300}{2250} \right]^2 \times 0.08 = 0.00142 \text{ square meters} \quad (11)$$

Hence, the received intensity is

$$P_{rdbm} = 39 + 10 \, Log_{10} \left[1.42 \times \frac{W}{M^2} \right] \quad (12)$$

$$P_{rdbm} = 39 + 10 \times 0.152288 + 10 \, Log_{10} \left[\frac{W}{M^2} \right] \quad (13)$$

$$P_{rdm} = 40.5 + 10 \, Log_{10} \left| W/M^2 \right| \quad (14)$$

Assuming the noise input at this rate has been previously determined for a 1.0 MHz bandwidth as -109 dbm this value would become for a 300 KH bandwidth in terms of the received signal strength in watts per square meter

$$\frac{S}{N} = 109 + 40.5 + 10 \, Log_{10} \left[\frac{W}{M^2} \right] \text{ db} \quad (15)$$

$$\frac{S}{N} = 149.5 + 10 \, Log_{10} \left[\frac{W}{M^2} \right] \text{ db} \quad (16)$$

A sample oscillograph trace of the received signal is shown in Figure 5. Figure 6 shows a comparison between the received signal and the predicted strengths.

Display Routine A routine is incorporated into the program, which causes Stromberg Carlson SC4020 cathode ray tube and an associated camera system to produce photographic records of the computed information. One example is the display of holes in the pattern at various gain levels. As discussed earlier, the areas above certain db levels are computed based on a unit radius sphere. Similarly, during execution of this routine those vector lengths which are greater than a given db level are marked with an asterisk, others are left blank. This procedure can be repeated as often as desired with a new picture being produced each time.

A picture is also taken of the plot of percent area greater than a given db level versus db level. A sample of this plot is shown in Figure 7.

Conclusion The results obtained to date indicate the feasibility of these digital methods as applied to antenna analysis. The work, here reported, appears to be only a threshold to more advanced techniques. Studies have already been initiated to remove some of the assumptions and move toward more exact solutions. Specifically, in the determination-of “look angles for spinning vehicles.

The program was designed for a particular vehicle - antenna system operating in conjunction with a given test range, future developments will incorporate means by which any antenna system on any range can be analyzed.

Another aspect of the visual analysis was to compare relative power levels and pattern structures under left and right hand polarization. This led to the conclusion that significant advantages can be achieved by use of diversity reception. Figure 8, shows a typical example of the degree of opacity which can be -achieved by diversity reception.

TABLE OF SYMBOLS

G	= gain in db’s
G'	= antilog of gain
θ	= aspect angle - degrees
ϕ	= roll angle - degrees
η	= efficiency index
A	= area - square units
R	= radius - linear units
P_R	= received power - watts
λ	= wavelength - meters/cycle
C	= speed of light - meters/second
f	= frequency - cycles/sec
W	= power - watts

LIST OF REFERENCES

Edward A. Wolff, “Antenna Analysis, “ John Wiley & Sons, Inc. New York, New York, 1967

F. E. Terman, “Electronic and Radio Engineering, “ McGraw Hill Book Company, Inc., New York, New York, 1955

Jasik, H. (Editor), “Antenna Engineering Handbook” McGraw Hill Book Company, Inc., New York, New York, 1961, Ch. 1 & 2

Kraus, John D., “Antennas, “ McGraw Hill Book Company, Inc., New York, New York, 1950, Ch. 1

Storer, James E. “The Impedance of an Antenna Over A Large Circular Screen, “ Journal of Applied Physics, Vol. 22, No. 8, 1951, pp 1058

J. S. Korsus, “Antennas, “ McGraw Hill Book Company, Inc. , New York, New York, pp 1; 1950

J. S. Hollis, “Antenna Measurements, “ Microwave Journal, Vol 3, No. 2, February 1960.

ACKNOWLEDGEMENTS

The author wishes to acknowledge the assistance of the following:

Mr. S. S. Kaye of Atlantic Research who coordinated the program.

Mr. F. Clarke Jr. , consultant, who assisted in the formulation.

Mr. J. E. Almanza of Atlantic Research who contributed to the formulation.

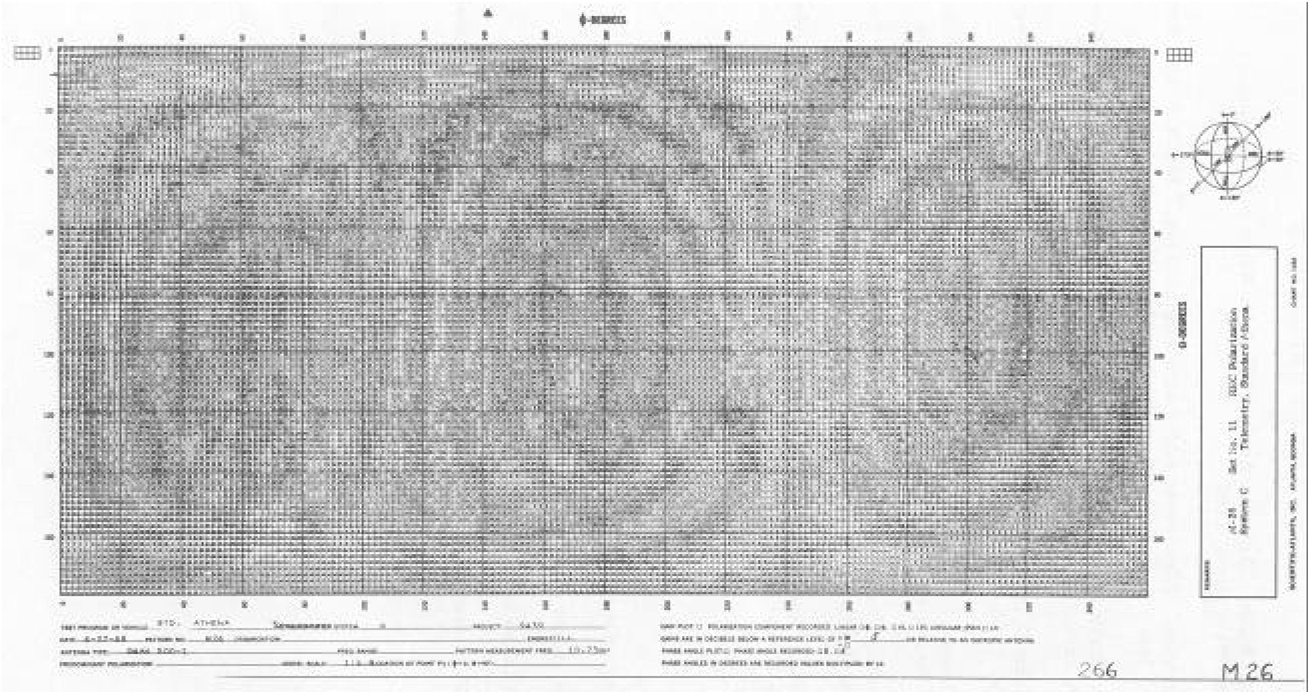

Figure 1. Typical Pattern Array

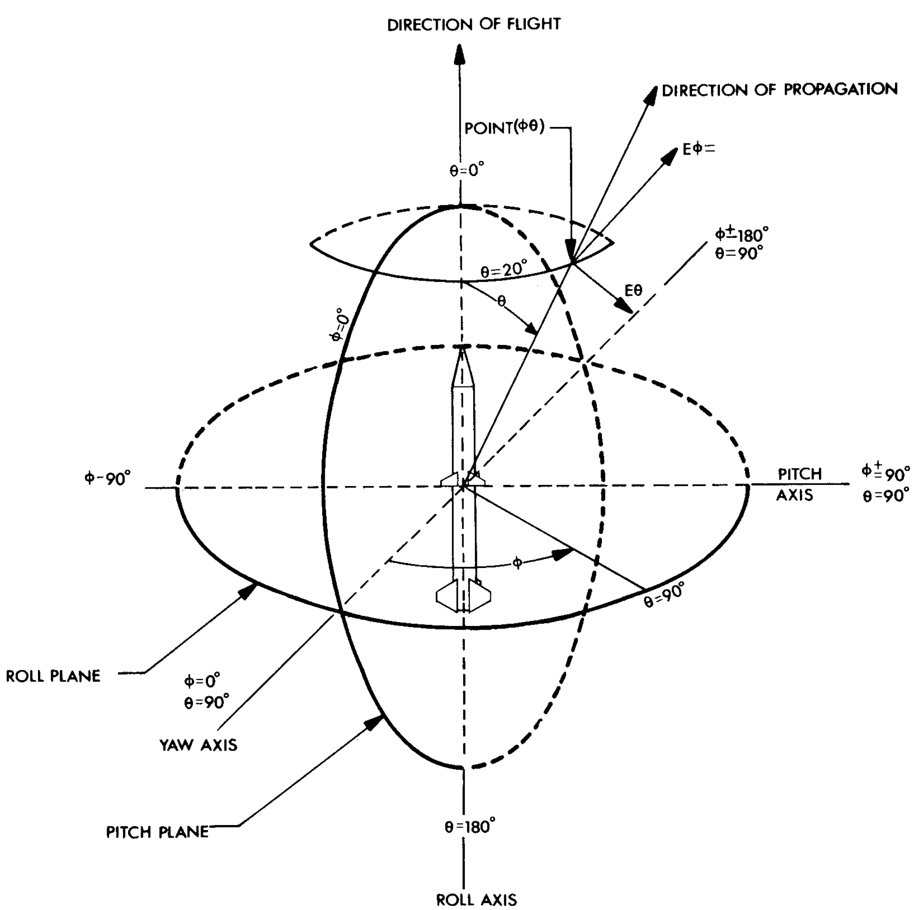

Figure 2. Orientation of Angles

```
ANTENNA PATTERN GAIN ANALYSIS

STANDARD ATHENA S-BAND TEST POD,SCALE 1/4.8 RHC

ANTENNA I.D. NUMBER =  M26              ISOTROPIC GAIN    =  -5.0  DB

OVERALL AVERAGE GAIN =              -7.113  DB

AVERAGE GAIN OVER FWD THIRD =       -6.660  DB

AVERAGE GAIN OVER MID THIRD =       -7.431  DB

AVERAGE GAIN OVER AFT THIRD =       -6.977  DB

ANTENNA EFFICIENCY                      19.442    PCNT

PERCENT AREA GREATER THAN

   GISO -16.0   GISO -15.0   GISO -14.0   GISO -13.0   GISO -12.0   GISO -11.0

     91.35        89.14        86.12        82.88        78.44        72.79

   GISO -10.0   GISO - 9.0   GISO - 8.0   GISO - 7.0   GISO - 6.0   GISO - 5.0

     65.03        56.46        46.75        33.98        21.88        13.79

   GISO - 4.0   GISO - 3.0   GISO - 2.0   GISO - 1.0   GISO -
      7.02         2.94         0.39         0.06

PCNT. GREATER THAN (GISO-8) FWD THIRD  =   50.99    (GISO-9) =   59.16     (GISO-10) =   66.45
PCNT. SMALLER THAN (GISO-8) FWD THIRD  =   49.01    (GISO-9) =   40.84     (GISO-10) =   33.55

PCNT. GREATER THAN (GISO-16) MID THIRD =   91.20   (GISO-17) =   93.17     (GISO-18) =   94.40
PCNT. SMALLER THAN (GISO-16) MID THIRD =    8.80   (GISO-17) =    6.83     (GISO-18) =    5.60

PCNT. GREATER THAN (GISO-8) AFT THIRD  =   49.34    (GISO-9) =   58.70     (GISO-10) =   66.18
PCNT. SMALLER THAN (GISO-8) AFT THIRD  =   50.66    (GISO-9) =   41.30     (GISO-10) =   33.82
```

Figure 3. Typical Computer Output Static Analysis

TRAJECTORY CASE NUMBER 31814 PAGE= 4

STANDARD ATHENA S-BAND TEST POD,SCALE 1/4.8 RHC

SITE NO 2 J-58 GR RIVER BH

ALTITUDE (ABOVE M.S.L.) = 4338.61 LAT = 38.98 LONG = -110.11 ORIENTATION ANGLE =0.0

TIME SEC.	ELEV ANGL	AZIM ANGL	ASPT ANGL	ROLL ANGL	GMIN DB	GMAX DB	GAVG DB	SLANT RANGE MILES	RECEIVED INTENSITY W/SQ.METS	PROBM DBM	S/N DB
0.53	0.53	141.95	107.20	360.00	-26.19	-2.00	-7.72	3.18	0.204786E-08	-54.4	53.1
1.01	0.78	141.97	107.03	360.00	-25.19	-2.00	-7.74	3.19	0.203362E-08	-54.4	53.1
2.01	1.80	142.04	107.82	360.00	-29.94	-2.00	-7.64	3.21	0.205212E-08	-54.4	53.1
3.98	4.88	142.21	115.27	360.00	-27.16	-2.27	-7.28	3.28	0.213938E-08	-54.2	53.3
4.48	5.76	142.26	117.00	360.00	-30.00	-2.00	-7.35	3.30	0.207415E-08	-54.3	53.2
5.48	7.63	142.38	118.98	360.00	-28.94	-1.51	-7.31	3.36	0.202023E-08	-54.4	53.1
6.98	10.70	142.60	123.65	360.00	-22.95	-2.00	-7.38	3.47	0.186123E-08	-54.8	52.7
7.48	11.78	142.68	125.19	360.00	-25.49	-2.00	-7.36	3.52	0.182367E-08	-54.9	52.6
8.48	14.00	142.85	127.91	360.00	-24.60	-2.00	-7.10	3.62	0.182759E-08	-54.9	52.6
9.98	17.38	143.13	132.48	360.00	-25.48	-2.00	-7.09	3.81	0.165640E-08	-55.3	52.2
10.48	18.51	143.23	134.02	360.00	-27.96	-2.00	-7.02	3.88	0.162273E-08	-55.4	52.1
11.48	20.72	143.43	136.90	360.00	-27.69	-1.90	-6.98	4.04	0.151119E-08	-55.7	51.8
12.98	23.91	143.76	141.05	360.00	-24.10	-2.00	-6.86	4.31	0.136572E-08	-56.1	51.4
13.48	24.94	143.87	142.39	360.00	-24.05	-2.00	-6.95	4.40	0.127788E-08	-56.4	51.1
14.48	26.92	144.09	144.98	360.00	-24.10	-2.00	-7.09	4.62	0.112680E-08	-57.0	50.5
15.98	29.71	144.44	148.63	360.00	-28.46	-1.68	-7.00	4.98	0.989782E-09	-57.5	50.0
16.48	30.59	144.56	149.79	360.00	-25.73	-1.11	-6.65	5.11	0.101805E-08	-57.4	50.1
17.48	32.26	144.80	152.00	360.00	-26.99	-2.00	-6.55	5.39	0.936971E-09	-57.8	49.7
18.98	34.58	145.15	155.08	360.00	-27.53	-2.00	-6.96	5.85	0.722891E-09	-58.9	48.6
19.48	35.30	145.27	156.04	360.00	-33.57	-2.00	-6.85	6.01	0.701156E-09	-59.0	48.5
20.48	36.65	145.51	157.86	360.00	-20.80	-2.00	-6.68	6.36	0.652091E-09	-59.4	48.1
21.98	38.50	145.86	160.38	360.00	-22.67	-2.19	-7.03	6.93	0.507374E-09	-60.4	47.1
22.48	39.06	145.98	161.16	360.00	-20.55	-2.58	-6.90	7.13	0.492945E-09	-60.6	46.9
23.48	40.13	146.20	162.64	360.00	-22.16	-2.32	-6.67	7.56	0.463726E-09	-60.8	46.7
24.98	41.56	146.54	164.66	360.00	-22.34	-0.67	-6.49	8.25	0.405882E-09	-61.4	46.1
25.48	42.00	146.65	165.29	360.00	-19.83	-0.35	-6.37	8.49	0.393051E-09	-61.6	45.9
26.48	42.82	146.86	166.48	360.00	-18.24	0.0	-6.23	9.00	0.361536E-09	-61.9	45.6
27.98	43.92	147.18	168.10	360.00	-19.14	-0.05	-6.29	9.82	0.299204E-09	-62.7	44.8
28.48	44.25	147.28	168.60	360.00	-19.89	-0.30	-6.68	10.11	0.258578E-09	-63.4	44.1
29.48	44.87	147.47	169.53	360.00	-21.30	-0.77	-7.19	10.71	0.204833E-09	-64.4	43.1
30.98	45.67	147.74	170.80	360.00	-23.45	-2.21	-7.71	11.63	0.153864E-09	-65.6	41.9
31.48	45.90	147.83	171.19	360.00	-27.53	-2.60	-7.77	11.94	0.144146E-09	-65.9	41.6
32.48	46.32	147.99	171.92	360.00	-35.21	-2.96	-7.53	12.57	0.137394E-09	-66.1	41.4
33.98	46.85	148.21	172.92	360.00	-30.00	-3.46	-7.37	13.51	0.123169E-09	-66.6	40.9
34.48	47.00	148.27	173.23	360.00	-30.55	-3.38	-7.29	13.83	0.119854E-09	-66.7	40.8
35.48	47.27	148.40	173.82	360.00	-33.20	-3.09	-7.07	14.46	0.115378E-09	-66.9	40.6
36.98	47.61	148.58	174.64	360.00	-28.26	-4.28	-7.77	15.40	0.865878E-10	-68.1	39.4
37.48	47.71	148.63	174.89	360.00	-25.95	-4.45	-8.04	15.71	0.782766E-10	-68.6	38.9
38.48	47.88	148.74	175.39	360.00	-21.52	-4.69	-8.45	16.33	0.659155E-10	-69.3	38.2
39.98	48.09	148.88	176.08	360.00	-22.77	-5.19	-8.93	17.25	0.528568E-10	-70.3	37.2
40.48	48.15	148.93	176.29	360.00	-22.12	-5.74	-9.43	17.55	0.454840E-10	-70.9	36.6
41.38	48.29	149.00	176.71	360.00	-20.88	-6.77	-10.29	18.11	0.350308E-10	-72.1	35.4
42.38	48.37	149.09	177.10	360.00	-19.69	-7.65	-11.02	18.70	0.277935E-10	-73.1	34.4
43.88	48.46	149.20	177.64	360.00	-19.38	-8.46	-11.84	19.59	0.209756E-10	-74.3	33.2
44.31	48.48	149.23	177.78	360.00	-20.00	-8.67	-12.02	19.84	0.196227E-10	-74.6	32.9
45.31	48.53	149.30	178.10	360.00	-20.41	-8.31	-12.25	20.42	0.175518E-10	-75.1	32.4
46.01	48.55	149.35	178.29	360.00	-19.25	-6.96	-12.16	20.83	0.172475E-10	-75.1	32.4
47.01	48.56	149.41	178.46	360.00	-18.38	-5.77	-12.03	21.41	0.167908E-10	-75.2	32.3

Figure 4. Typical Computer Output Radar Tracking Information

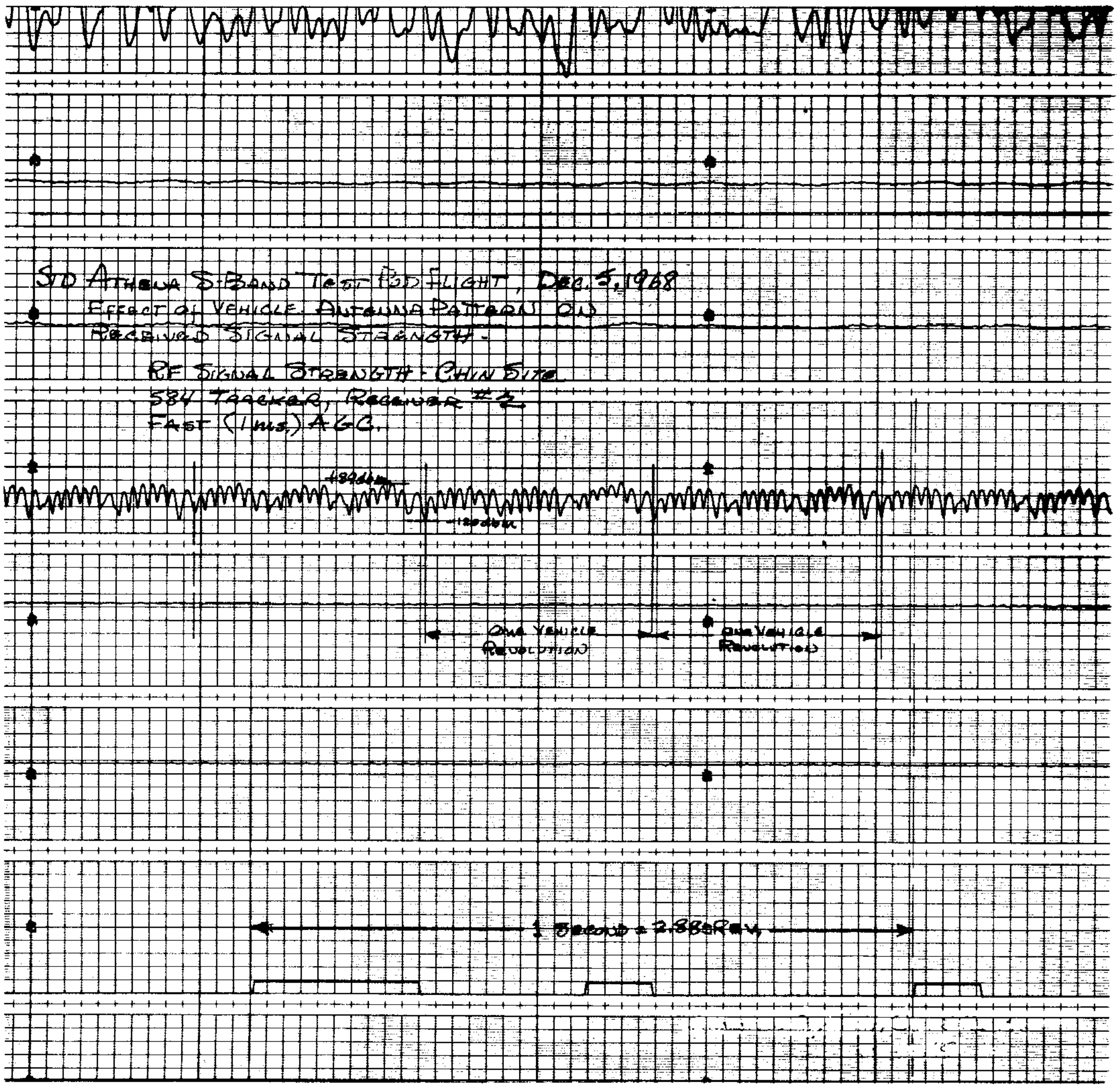

Figure 5. Flight Data Detail

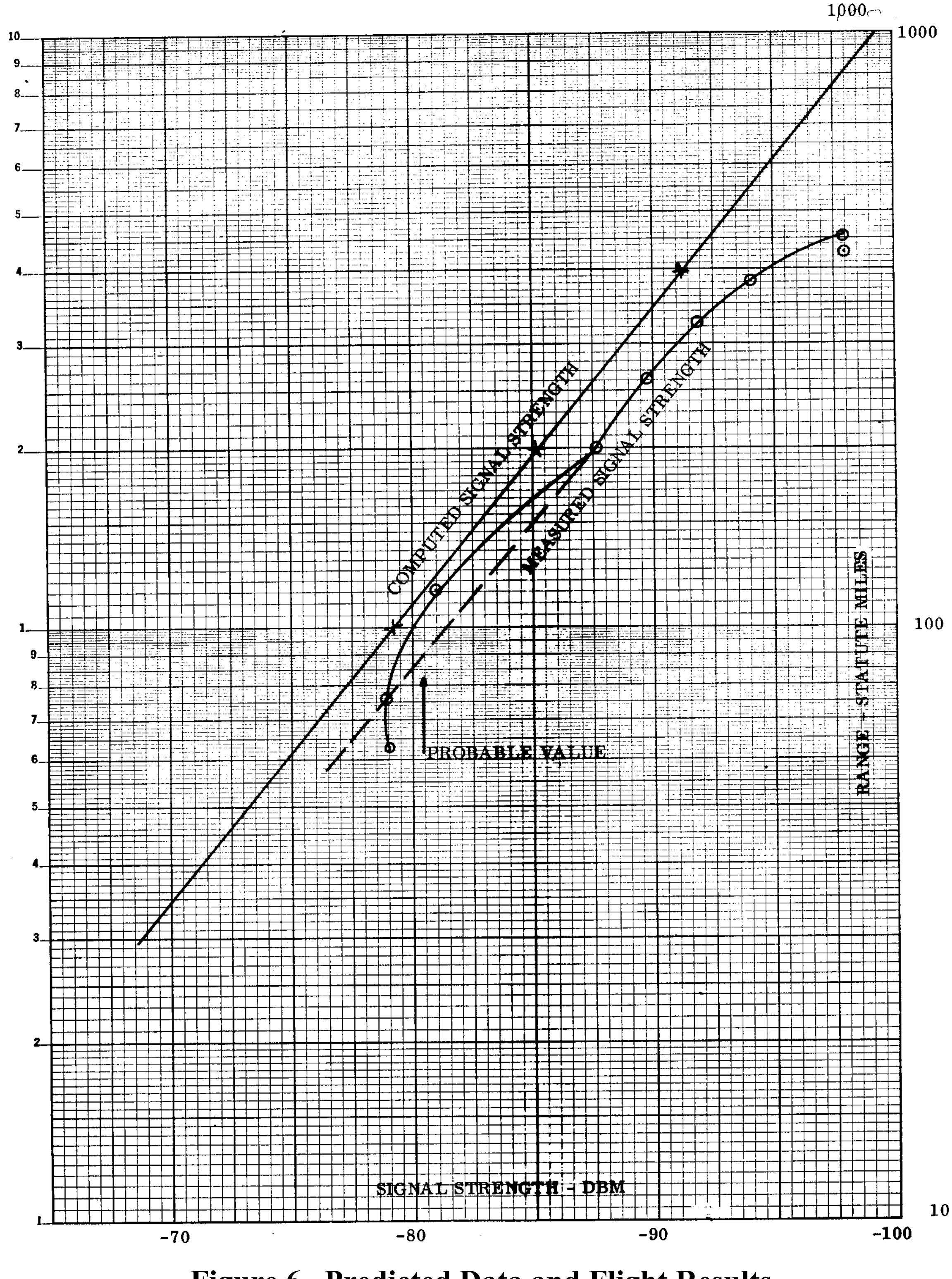

Figure 6. Predicted Data and Flight Results

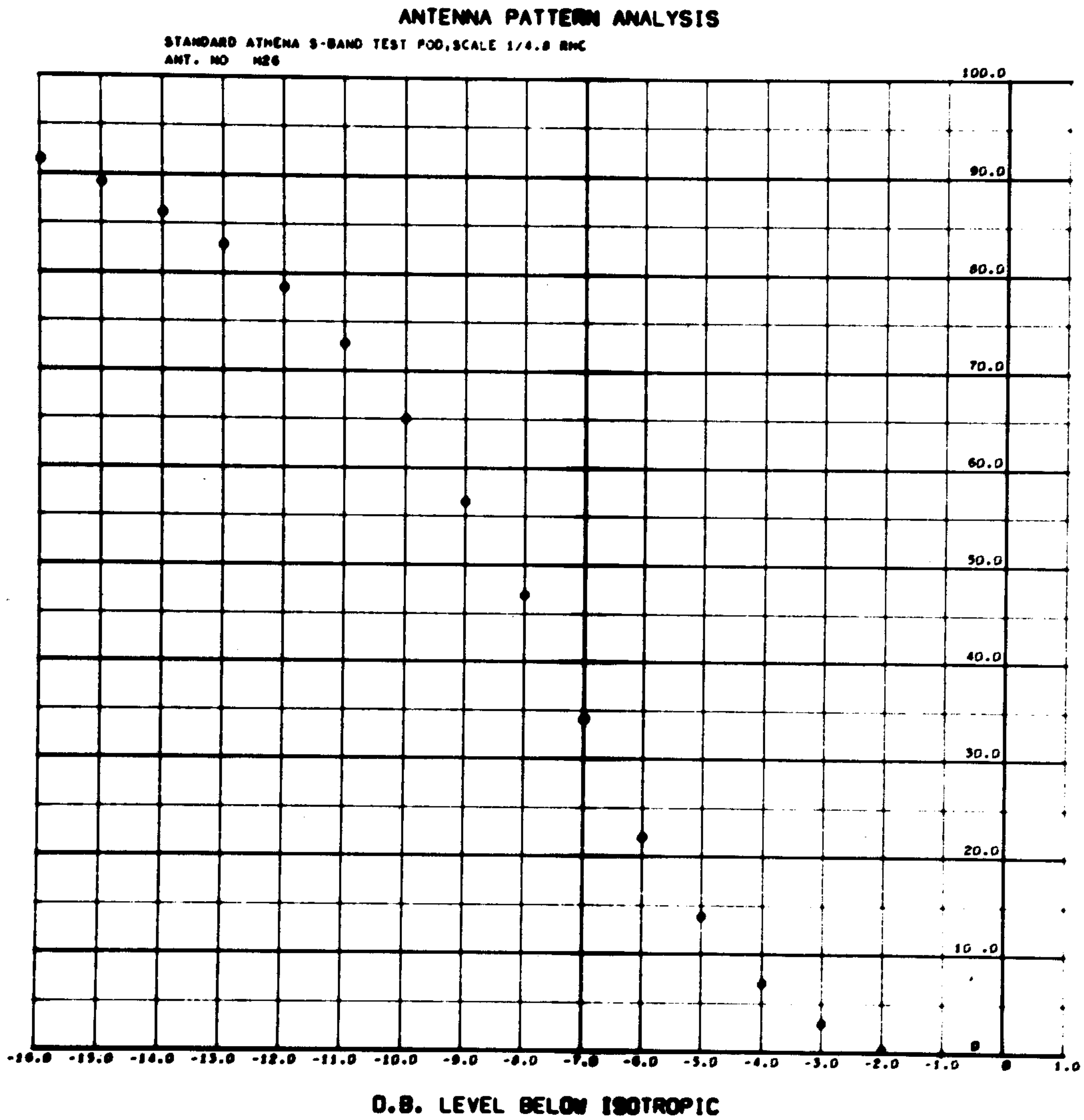

Figure 7. Typical Area vs Gain Plot

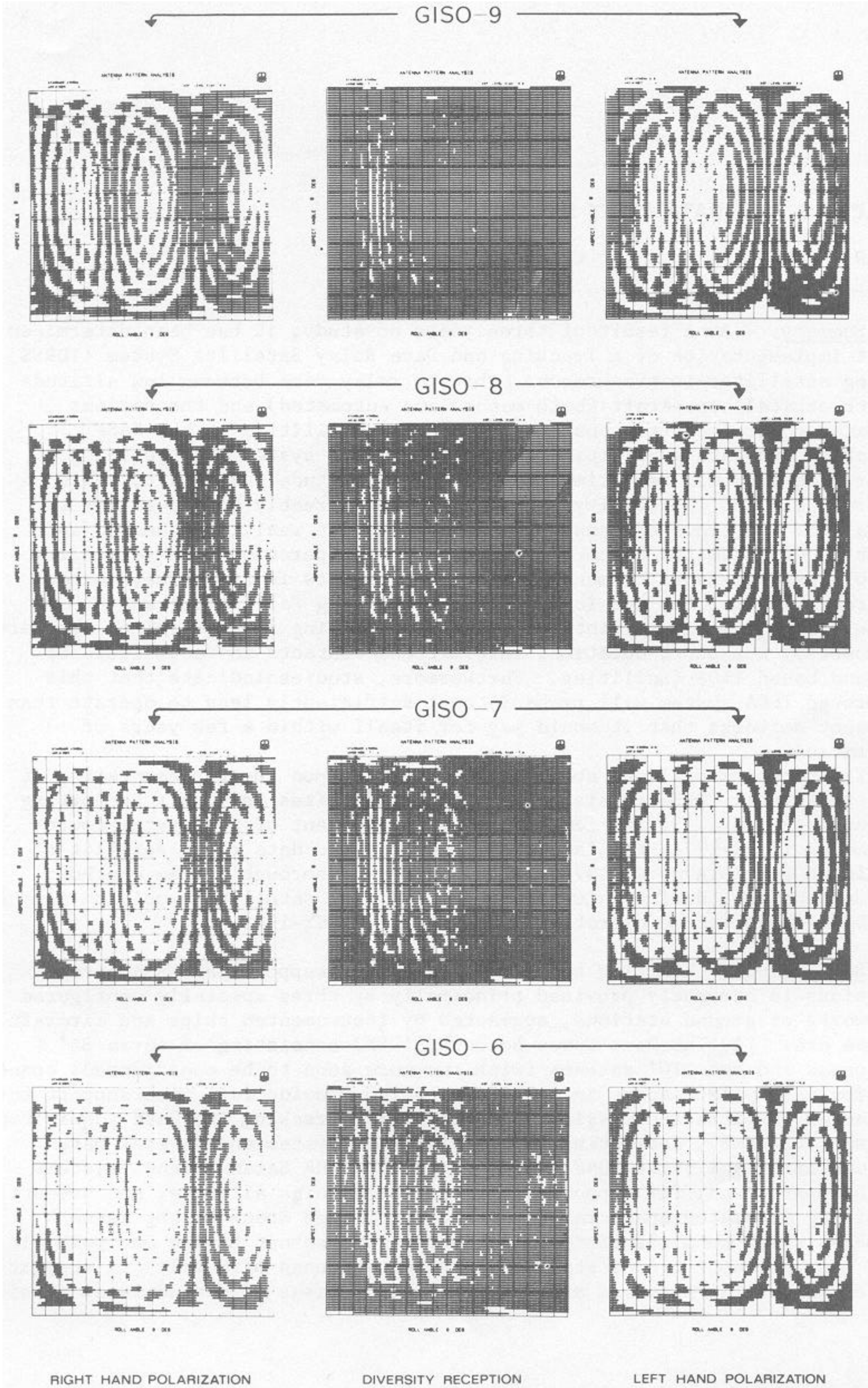

Figure 8. Typical Pictorial Display